The effect of mean stress on the fatigue behaviour of overhead conductor function of the *H/w* parameter

Remy Badibanga[1,*], *Thiago* Miranda[1], *Pedro* Rocha[1], *Jorge* Ferreira[1], *Cosme* da Silva[1], *José* Araújo[1,*].

[1]UnB, University of Brasília, Department of mechanical Engineering, CEP 70910-900

Abstract. The objective of this work is to evaluate the effects of mean stress on the fatigue behaviour of an All Aluminium Conductor (AAC Orchid), Aluminium Conductor Steel Reinforced (ACSR Tern), and an Aluminium Conductor Alloy Reinforced (ACAR 750 MCM). In this sense, 72 fatigue tests on overhead conductors were performed using different values of *H/w* parameter. Based on the experimental results, the parameters which describe the fatigue behaviour of the conductors were determined after generating theirs S-N curves. In the assessment of the mean stress effects on the fatigue life, Goodman and Gerber's relations were fitted to evaluate the use of such models for the conductors. It was observed that the evaluation of the mean stress effect on the overhead conductor could be made by using the fatigue relations.

1 Introduction

The overhead conductor is the only part carrying electricity, so its contribution has been estimated as carrying up to 40% of all power line transmission costs. However, this transmission line is susceptible to wind, snow, earthquakes and other weather conditions [1]. Aeolian vibration is the main cause of conductor fatigue failure, especially at devices which restrain its movements [2-4]. Frequently, the observed fatigue failures on overhead conductors occurs near or inside the suspension clamp devices, where there are many loads acting on the assembly conductor/clamp [5,6]. Among the loads, there are the stretching load of the conductor, the bending displacement due to the Aeolian vibration which generates the bending stress and the clamping torque.

The control of the stretching tension of conductors at the design stage has been a concern for many years [1]. One of the reasons is that the tension of conductors during the most severe climate period should not exceed the allowable tension of the conductor. Also, the stretching tension must be controlled in order to restrict the violation of the line clearance and also to protect the conductor against the harmful Aeolian vibration. It is well-known that an overhead conductor becomes more vulnerable to Aeolian vibration when its tensile tension increases. Therefore, the *Conseil International des Grands Électriques* (International Council on Large Electric Systems), abbreviated CIGRÉ, has found necessary to establish an upper limit for conductor tension that can prevail for a significant period of time. The Every Day Stress (EDS) panel was created by CIGRÉ to investigate the safe parameter design of power line conductors [7,8]. The EDS is the maximum tension load to which the conductor can be subjected, at the temperature which will occur for the longest period of time in one year, without any risk of damage from Aeolian vibrations. It is expressed in percentage of the ultimate tensile tension of the conductor, and CIGRÉ has fixed its values according to the type of the conductor. However, failure on overhead conductors due to Aeolian vibration has been observed in situ even when the transmission line has been designed with the recommended EDS value. For instance, a survey conducted by CIGRÉ revealed that 78% of lines failed by fatigue before 20 years after their launching [8]. Thus, such a kind of study makes it clear the need of another parameter to design the lines against fatigue

The *H/w* parameter has recently been suggested by CIGRÉ to better explain and describe the fatigue damage occurring on power line conductors due to the Aeolian vibration. The tenants of this parameter suggest that all overhead conductors stretched with the same value of *H/w* will have a similar fatigue life [9]. Although, no experimental laboratory on overhead conductors was performed to corroborate this idea. After a thorough literature investigation, some publications have been identified regarding fatigue of power lines related to the EDS parameter [1,5,6]; however, there are few publications related to the *H/w* parameter. This present work, then, has the objective of conducting an experimental campaign to access the effect of the mean stress on the fatigue behaviour of conductor tested under different values of *H/w* parameter. Seventy two (72) fatigue tests were carried out on three types of conductors, namely an All Aluminium Conductor (AAC Orchid), Aluminium Conductor Steel Reinforced (ACSR Tern), and an Aluminium Conductor Alloy Reinforced (ACAR 750 MCM). Additionally, the mean stress,

* Corresponding author: badibanga12@gmail.com jaaunb@gmail.com

which is function of *H/w*, and the bending stress (Poffenberger Swart stress) were fitted through different prediction models of the mean stress effect.

2 Bending stress and *H/w* parameter

2.1 Bending stress

The main cause of fatigue failure of strands in overhead conductors is Aeolian vibration, a fatigue which generally occurs at points where conductor motion is constrained against transverse vibration, such as at suspension clamps. During Aeolian vibration, the conductor undergoes cyclic movement which induces bending stress in power line conductor wires.

Most fatigue failures in strands of conductors occurs in the suspension clamp at the contact points of wires-to-wires and wires-to-suspension clamp [1,10]. Because of the difficulty on accurate measurement of mechanical strain or stress at these points, the adoption of some assumptions is vital. A mathematical model was developed by Poffenberger and Swart [11] to calculate the bending strain or stress in the outer layer of the conductor's aluminium wire. This mathematical model considers the cable, near the suspension clamp, as an Euler beam (Fig.1).

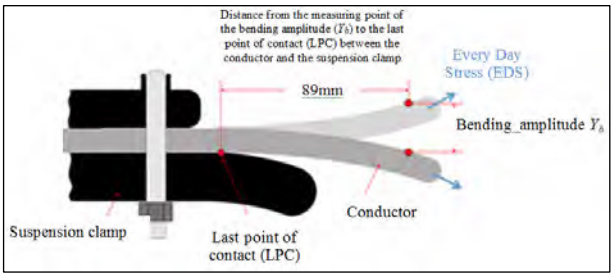

Fig. 1. Schematic montage of the conductor and the suspension clamp showing the standard position to measure the bending amplitude

Thus, the vertical amplitude, measured peak-to-peak at 89 mm (3.5 in) from the last point of contact (LPC) between cable and suspension clamp, can be converted to the bending strain or stress in the outer layer of the aluminium wire conductor using Eq. 1. The Poffenberger-Swart Equation has been developed as follows:

$$\sigma_a = KY_b \tag{1}$$

where σa is the dynamic bending stress amplitude (0-to-peak); Y_b is the conductor's vertical amplitude range (peak-to-peak) measured at 89 mm from LPC; and:

$$K = \frac{E_a d p^2}{4(e^{-px} - 1 + px)} \tag{2}$$

where E_a (MPa) is the aluminium Young's modulus; d (mm) is the diameter of wire in the outer layer; x is the distance on the conductor from the LPC (between the conductor and the suspension clamp) and the vertical displacement measuring point, (usually x = 89 mm), as one can see on Fig 1; and:

$$p = \sqrt{\frac{T}{EI}} \tag{3}$$

where T (N) is the static conductor tension at average ambient temperature during test period; and EI (N.mm2) is the flexural stiffness of the conductor, whose minimum value is as follows:

$$EI_{min} = n_a E_a \frac{\pi d_a^4}{64} + n_s E_s \frac{\pi d_s^4}{64} \tag{4}$$

where n_a, E_a, d_a are the number, individual diameter and Young's modulus of the aluminium wires; and n_s, E_s, d_s are the respective values for the steel wires. In this approach, the conductor is considered as a bundle of individual wires free to move relative to each other; the flexural stiffness takes its minimum value, EImin. For smaller bending amplitudes, the individual wires would stick together; thus the conductor would behave as a solid rod, increasing the flexural stiffness to its maximum. Formulae that consider the stick-slip theory to compute EI and hence the dynamic bending stress were proposed by Papailiou [12,13].

2.2 *H/w* parameter

The design of overheard power lines has been guided by the control of the conductor tension. Many reasons have justified this option: among them is the objective of ensuring that the maximum tension of the conductor corresponding to the assumed most severe climatic loading does not exceed a predefined load. Another reason is related to the maximum operation temperature of the conductor, which could allow it to work with respect to the conductor safe clearance. It is well-known that the conductor becomes increasingly vulnerable to Aeolian vibration when its static tension increases. Therefore, it is necessary to establish an upper limit for conductor tension that can prevail for a significant period of its lifetime. Consequently, the Every Day Stress (EDS) panel was created by CIGRÉ to investigate a limiting parameter capable to safely design line conductors against fatigue due to Aeolian vibration. Many parameters have been proposed for the safe design of overhead conductors, but two – Every Day Stress and the catenary parameter *H/w* – are the most prevalent in the literature.

The Every Day Stress (EDS) parameter was initially proposed by CIGRÉ in 1960 [9]. The EDS, expressed as a percentage of the conductor rated tensile stress (RTS), is defined as the maximum tensile load to which the conductor can be subjected, at the temperature which will occur for the longest period of the time without any risk of damage due to Aeolian vibrations. CIGRÉ recommends different values of EDS for overhead conductors and for conductors with dampers only, armor rods only, as well as for conductors with both dampers and armor rods. However, field observations have reported fatigue of power lines after the application of the recommended EDS values by CIGRÉ [1,7,9].

Consequently, the EDS parameter appears to be insufficient for explaining the recent damage found on power lines. Clearly, the requirement for a new parameter is evident.

Another parameter adopted by CIGRÉ, is defined as the ratio between the initial horizontal tensile load (*H*) and the conductor weight (*w*) per unit length, *H/w*; this parameter is also called the catenary parameter. The tensile load (*H*) is the initial horizontal tension before any significant wind and ice loading and before creep at the average temperature of the coldest month at the site of the power line [1,7]. Compared to the EDS, the *H/w* presents several advantages, as it affects a number of parameters involved in the fatigue characteristic of conductors. One of them is that the *H/w* parameter takes into account the diameter of the power line conductor, which influences the energy induced by the wind and the frequency of vortex formation [7,9].

3 Materials and methods

3.1 Materials

Three conductors named AAC Orchid, ACSR Tern and ACAR 750 MCM were chosen for this work, thereafter the fatigue behaviour of conductors was investigated. The AAC Orchid is a conductor composed only of aluminum wires Al 1350 H19, the ACSR Tern cable has steel core (7 wires) and two layers of Al 1350 H19 aluminum wires, and cable ACAR 750 has aluminum alloy core (Al 6201 T81) and the wires from external layers are made of Al 1350 H19 aluminum. The basic characteristics of these conductors are presented in Table 1.

Table 1. Mechanical and geometrical properties of the three conductors

		AAC Orchid	ACSR Tern	ACAR 750 MCM
Conductor diameter (mm)		23.3	27.03	25.32
Number of wires on each layer	*Aluminium*	18-12-6-1	21-15-9	18-12-6-1
	Steel	-	6-1	-
Diameter of wires (mm)	*Aluminium*	3.33	3.38	3.617
	Steel	-	2.25	-
Linear mass (kg/m)		0.889	1.339	1.046
Rated tensile strength (kgf)		5143	10010	8635

3.2 Strategy to evaluate the adherence of the mean stress models.

The strategy used to evaluate the adherence of the fatigue models consist of the use of three parameters that characterize a mechanical fatigue behavior: the mean stress, S_m, alternating stress, S_a, and the resulting life, *N*. As shown in Fig. 2, the application of the data that characterize the mean and alternating stress in one mean stress model allows to evaluate theirs effect on the fatigue behavior. The evaluation of the mean and the alternating stress is made by extrapolating the S-N equation when $S_m = 0$ and the equivalent fatigue strength, S_{ar} Model, to the specific fatigue model. In a similar way, the application of the fatigue life, *N*, in the Basquin's equation allows the estimation of the new value for the equivalent endurance limit, called S_{ar} Basquin. If the prediction model correlate well to the experimental results then the values of S_{ar} Model and S_{ar} Basquin should be identical statistically. The equations used to estimate the equivalent alternating stress, S_{ar} Model are shown in Eq. 5-6, which correspond respectively to Goodman and Gerber´s models.

$$S_{ar} = \frac{\sigma_a}{1-(\frac{\sigma_m}{S_{rt}})} \quad (5)$$

$$S_{ar} = \frac{\sigma_a}{1-\left(\frac{\sigma_m}{S_{rt}}\right)^2} \quad (6)$$

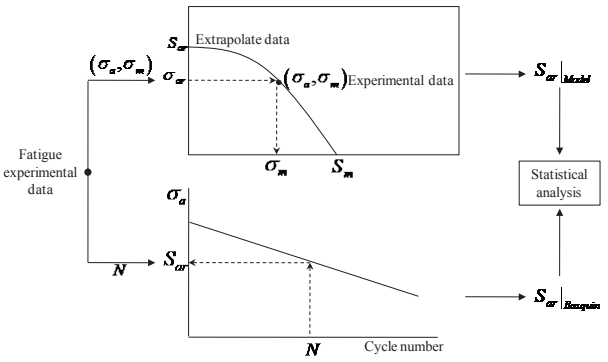

Fig. 2. Strategy used to evaluate the adherence of the mean stress models**.**

4 Experimental procedure

At the GFFM (Fatigue, Fracture and Materials Research Group) laboratory (University of Brasília), three similar resonance fatigue test benches of conductors were used. A brief description of the bench is provided below as it was previously described in other publications [2,5,14]. Each bench has a length of 46 m divided in two spans – the active and the passive span – which have, respectively, 40 and 6.8 m. The scheme of the three benches is shown in Fig. 3(a), while Fig. 3(b) represents the benches side view. The test starts by anchoring the conductor on the two fixed blocks (fixed blocks 1 and 3) and thereafter mounting the suspension clamp on the support which is rigidly fixed on the adjustable block 3. The conductor is stretched at the recommended value of *H/w* through the strain clamp by using the hand traction winch and weight. To simulate the vibration, an electrodynamic shaker is connected to the conductor via device which allows a good alignment between the shaker and the conductor axes. A wire break detector is attached to the conductor at the first node of

the conductor from the suspension clamp toward the shaker.

All fatigue tests were performed according to IEEE (Institute of Electrical and Electronics Engineers) and CIGRÉ standards which establish the criterion to stop the conductor´s fatigue test when the number of strands broken is 10% of the total number of conductor aluminium wires [15,16]. To measure the bending stress of the conductor, three strain gauges were glued on the most upper conductor's wires (being one strain gauge by wire) diametrically opposed to the LPC between the suspension clamp and the conductor. The bending displacement peak-to-peak (Y_b) measured at 89 mm from the LPC between the conductor and the suspension clamp was controlled, along with the vibration frequency, during all fatigue tests. For each conductor, the S-N graph was generated by performing nine fatigue tests (three bending stress and three tests by bending stress). The three levels of bending stress considered during the experimental program and the corresponding bending displacement peak-to-peak generated by applying the Poffenberger-Swart constant (K) are presented in Table 2 for the three values of *H/w* parameter.

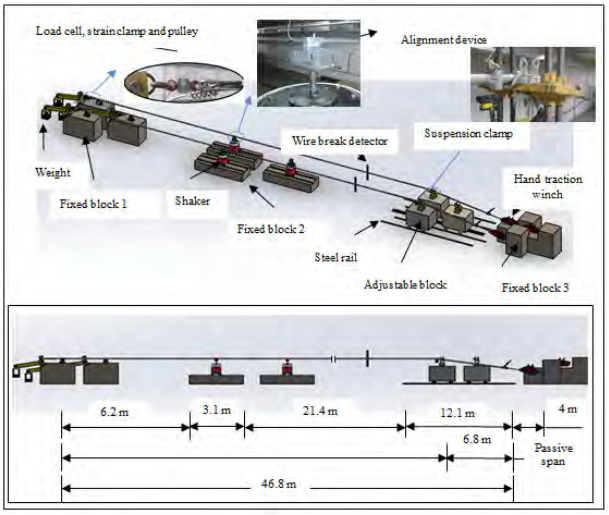

Fig. 3. Three fatigue test benches for overhead conductors at the University of Brasilia: (a) overall three dimensional view and (b) side view

Table 2. The bending amplitude (Y_b) at 89 mm from the LPC between the suspension clamp and the conductor and the Poffenberger-Swart constant (K) calculated using Eq. 1 and Eq. 2 for different conductors at a specific mean stress.

Conductor	*H/w* [m]	*K* [MPa/mm]	Poffenberger-Swart stress [MPa]		
			26.8	**28.22**	**31.35**
ACSR Tern	1820	32	0.84	0.88	0.98
	2144	33.66	0.80	0.84	0.93
	2725	36.38	0.74	0.78	0.86
AAC Orchid	1820	30.91	0.87	0.91	1.01
	2144	32.49	0.82	0.87	0.96
	2725	35.07	0.76	0.80	0.89
ACAR 750 MCM	1820	31.98	0.84	0.88	0.98
	2144	33.53	0.80	0.84	0.93
	2725	36.09	0.74	0.78	0.87

5. Results and discussions

5.1 Fatigue tests

A total of seventy-two tests were performed to generate nine S-N curves under three values of *H/w* parameter. Each *H/w* value is related to the mean stress of the conductor as shown experimentally by Kalombo et al [17]. For each conductor, 24 fatigue tests were performed, nine tests with *H/w* value of 1820 m; nine tests with *H/w* = 2144 m; and six tests with *H/w* = 2725 m. Figures 4-6 present the S-N curves obtained by means of the experimental procedure presented in the preview section. In these graphs, the results are grouped by *H/w* value and the dependent variable, the fatigue life *N*, Number of cycles, is plotted in abscissa on a logarithmic scale and the independent variable, Poffenberger-Swart stress (Expressed in MPa), is plotted on the ordinate, also on logarithmic scale. The fatigue test was stopped when the number of wires broken is equal to either three or 10% of the total number of aluminium wires, whichever is greater [16].The synthesis of the results obtained from the above experimental procedures is presented in Table 3. The S-N curves of the three conductors tested at the same value of *H/w* = 1820 m are shown in Fig. 4. Meanwhile, Figs. 5-6 present respectively the graphs correspond to the fatigue curves behaviour of the conductors tested with the *H/w* value equal to 2144 and 2725 m.

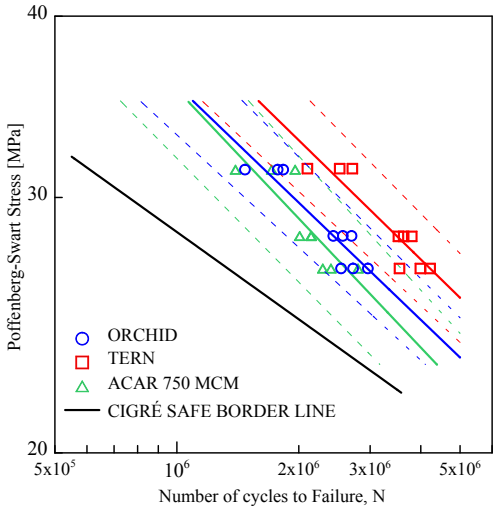

Fig. 4. S-N graphs of different conductors tested with the same value of H/w =1820 m.

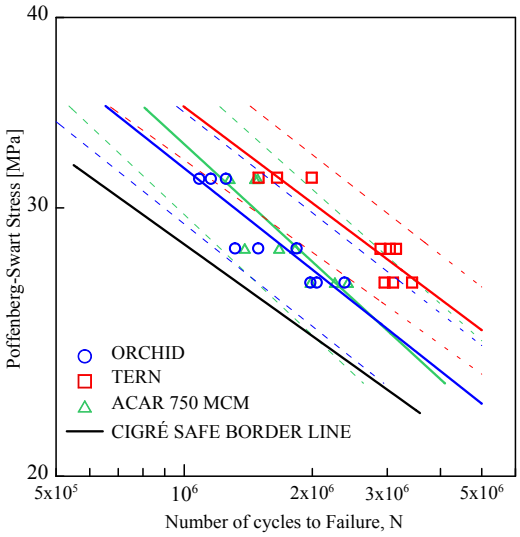

Fig. 5. S-N graphs of different conductors tested with the same value of H/w = 2144 m.

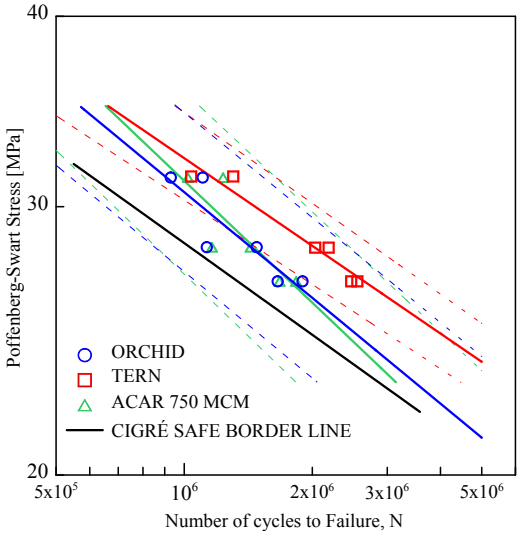

Fig. 6. S-N graphs of different conductors tested with the same value of H/w =2725 m.

In order to evaluate the accuracy level of the process of obtaining the S-N curves, whose parameters are listed in the Tables 3, the dispersion diagram was constructed (Fig. 7). This figure relates the experimental fatigue life observed for each conductor tested, N, with the estimated fatigue life calculated from the S-N relationships, N_{test}. In the graph of Fig. 7, the dashed lines and dot-dash lines parallel to the one that passes through the origin (perfect correlation) represent respectively a range of life variations with factors of 1.5 and 3. The graph presented in Fig. 7 shows that the prediction based on the CSBL (CIGRÉ Safe Border Line) is the most conservative one, as presented by CIGRÉ [1,16]. Additionally, the predictions based on the S-N curves represented in Table 3 showed a strong correlation between the observed and the respective expected lives. In general, the predicted values are distributed symmetrically around the perfect correlation line.

Table 3. The synthesis of the experimental results conducted on different conductors

Conductor	H/w (m)	S_m (MPa)	$S_a = AN^b$	
			A	b
AAC Orchid	1820	48.3	1.88E+04	-0.443
	2144	56.9	5.80E+03	-0.372
	2725	72.3	1.45E+03	-0.278
ACSR Tern	1820	48.3	4.70E+03	-0.340
	2144	56.9	1.72E+03	-0.277
	2725	72.3	9.74E+02	-0.244
ACAR 750 MCM	1820	48.3	9.75E+03	-0.401
	2144	56.9	3.71E+03	-0.339
	2725	72.3	3.87E+03	-0.347

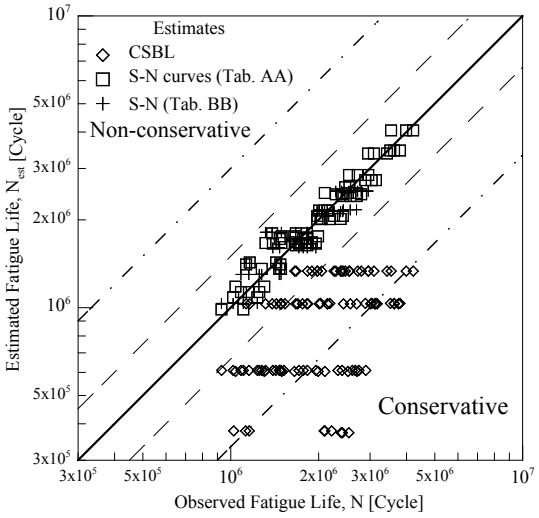

Fig. 7. Accuracy of the fatigue life predictions obtained from the experimental S-N curves of conductors with respect to the CSBL (CIGRÉ safe border line).

5.2 Adherence of the models to the experimental results

The comparisons are made between the predicted models of the mean stress effect by considering the experimental lives obtained in section 3.1 (Fig. 8). These graphs show the dispersion diagrams which correlate the observed fatigue lives and the respective fully reversed equivalent stress estimated by Goodman and Gerber's model, respectively. In addition, the S-N curves that best represent each model is also plotted. Thus, replacing the terms representing the fatigue strength limit for the reverse loading condition in Eq. 7, the function describing the Goodman and Gerber's models will take the form of the expression presented in Eq. 8 when $k = 1$, the function represents the Goodman's model and when $k = 2$, the function represents the Gerber's model.

$$S_{ar} = AN^{b} \tag{7}$$

Where A and b are respectively the constant and the exponent of the Sar-N curves.
From Eq. (7) and the fatigue models Eq. 5-6, the fatigue life was estimated using the following equation:

$$N = \left[\frac{1}{A}\left(\frac{\sigma_a}{1-\left(\frac{\sigma_m}{S_{ut}}\right)^{k}}\right)\right]^{\frac{1}{b}} \tag{8}$$

The analysis of the results from Table 4, which summarizes the results of the non-linear regression process of the experimental data, shows that the models to estimate the mean stress effect of the fatigue resistance of overhead conductors had the same capacity to correlate a fully reversed equivalent stress, S_{ar}. Despite having very different adjustment parameters in terms of the fit quality of the analyzed models (quantified by r^2), the experimental fatigue life shows that the correlation coefficient has a value of 0.5, with small marginal variations between the two models.

A significant part of the experimental points related to the AAC Orchid and ACAR 750 MCM conductors are positioned to the left of the trend curves, indicating that the fatigue failure occurred with the number of cycles which is smaller than the one expected. This position of the experimental points indicates that the predictions are non-conservative. However for the ACSR Tern conductor, the experimental points were positioned to the right of the trend curves (in this case the predictions are conservative). This characteristic in the distribution of the results also helps to explain the deviation from the trend curve of the lines representing the boundaries of the mean response prediction interval. The analysis of the graphs presented in this figure indicates that, regardless of the model used, all prediction were within the region bounded by the bands of variation of two lives.

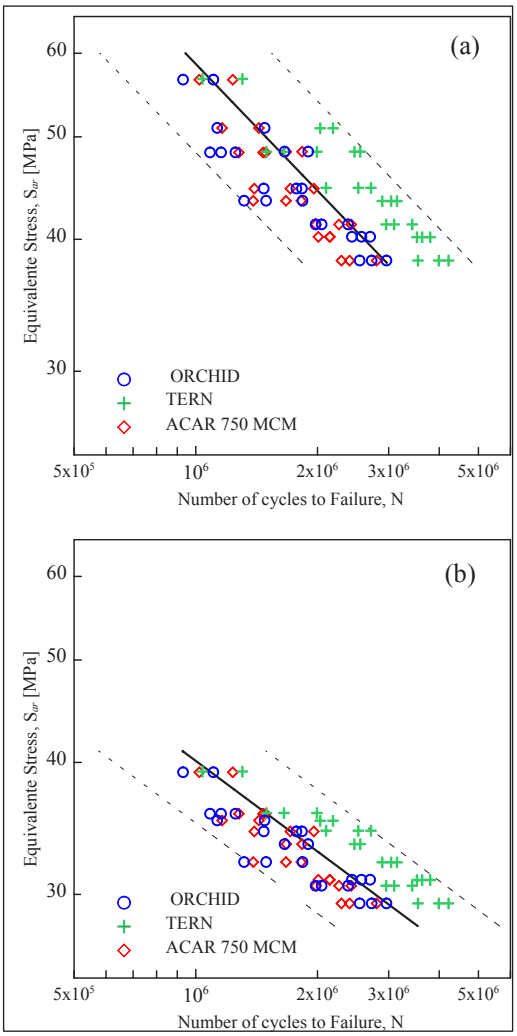

Fig. 8. Comparison between the experimental fatigue lives, N, and the fully reverse equivalent stress amplitudes, S_{ar}, predicted by various fatigue models: (a) Goodman, (b) Gerber

Table 4. Stress-life fitting constants with the correlation coefficient r^2

Model	S-N Curve Parameter		r^2
	A[MPa]	b	
Goodman	1.13E+04	-0.381	0.55
Gerber	2.80E+04	-0.435	0.49

6. Conclusions

In the present publication, the fatigue behavior of the three conductors named AAC Orchid, ACSR Tern and ACAR 750 MCM are presented using the *H/w* value of 1820, 2144 and 2725 m. The S-N curves were generated using three values of *H/w* which correspond to the following values of mean stress (48.30, 56.89 and 72.31 MPa). Thereafter the comparison was done between the Basquin alternate stress and different fatigue models. The mean stress effect was predicted using the Goodman and Gerber's models. Based on the results presented, the following conclusions could drawn:

- The fatigue life of conductors is strongly influenced by the mean stress which is a function of the *H/w* value;
- Using Goodman and Geber´s fatigue models, most of the estimates for our experimental data fell within a factor two bandwidth.
- The Goodman and Geber´s fatigue models were more conservative to estimate the mean stress on the AAC Orchid and ACAR 750 MCM conductors.

Acknowledgements

The authors would like to acknowledge the financial support of TAESA, ATE II, ATE III, EATE, TME, AETE, TBE and Brasnorte for this research (Grant no. 4600001511) by means of the R & D program of ANEEL. The support of Finatec is also acknowledged.

References

1. J. Chan, *Transmission Line Reference Book: Wind-Induced conductor motion* (EPRI, Palo Alto, California, 2006)
2. A.A. Fadel, D. Rosa, L.B. Murça, J.L.A. Ferreira, and J.A. Araújo, Int. J. Fatigue **42** 24-34 (2012)
3. IEEE, *Guide for Aeolian Vibration Field Measurements of Overhead Conductors* (2007)
4. A. Cardou, L. Cloutier, M. St-Louis, A. Leblond, Standardisation of Fretting Fatigue Test Methods and Equipment. 231-242. (1992)
5. V.F. Volker, R.B. Kalombo, R.M.S. Cosme, M.N. Nogueira, J.A. Araújo, Electr. Pow. Syst. Res **116** 346–358 (2014)
6. G.E. Ramey, R. R., Duncan, R.M. Brunair, J. Energ **112** 138-151 (1986)
7. CIGRÉ Report 273, *Overhead conductor safe design tension with respect to aeolian vibrations* (Task Force B2.11.04, CIGRÉ, 2005)
8. CIGRÉ, *Engineering Guidelines Relating to Fatigue Endurance Capability of Conductor-clamp Systems* (SC B2, CIGRÉ, 2010)
9. J.S. Barrett, Y. Motlis, IEEE Proc. Gener. Transm. Distrib **148** 54-59 (2001)
10. W.G. Fricke, C.B. Rawlins, IEEE Trans. Power Appar. Syst **87** (1968)
11. J.C. Poffenberger, R.L. Swart, IEEE Trans. paper **84** 281-289 (1965)
12. K.O. Papailiou, IEEE Trans. Power Del. **12** 1576-1588 (1997)
13. K.O. Papailiou, CIGRÉ, SC 22 WG11, (1995).
14. C.R.F. Azevedo, A.M.D. Henriques, A.R. Pulino Filho, J.L.A. Ferreira, J.A. Araújo, Eng. Fail. Ana **16**, 136-151 (2009)
15. IEEE Std 1368 (2007)
16. CIGRÉ WG 04 SC 22 - 02, **63** (1979)
17. R.B. Kalombo, M.S. Pestana, J.L.A. Ferreira, C.R. M. da Silva, J.A. Araújo, Tribol. Int **108** 141–149 (2017)